Phase-Separation Kinetics of Mixtures of Linear and Star-Shaped Polymers

Bradford J. Factor, Thomas P. Russell,* and Barton A. Smith

IBM Research Division, Almaden Research Center, 650 Harry Road, San Jose, California 95120-6099

Lewis J. Fetters

Exxon Research Laboratory, Annandale, New Jersey 08801

Barry J. Bauer and Charles C. Han

National Institute of Standards and Technology, Gaithersburg, Maryland 20899

Received January 5, 1990; Revised Manuscript Received March 6, 1990

ABSTRACT: The phase separation of mixtures of four-armed star polystyrene with linear poly(vinyl methyl ether) was investigated by time-resolved light scattering. It was found that the kinetics of phase separation was essentially the same as that of the corresponding mixtures of linear polymers. The effect of chain topology was evident only when the molecular weights of the individual arms were large. This resulted in a reduced rate of phase separation. The linearized Cahn–Hilliard–Cook theory of spinodal phase separation qualitatively described the features of the experiments; however, the scattering vector dependence of the amplification factor deviated from the expected behavior.

Introduction

The kinetics of phase separation in polymer mixtures has been the subject of intense experimental[1-6] and theoretical[7-12] investigation. Despite the complex nature of the diffusive motion of polymers, the kinetics of the initial stages of phase separation in polymer mixtures appears to conform to a relatively simple linearized model first developed by Cahn,[13] Hilliard,[14] and Cook.[15] This model was initially proposed to describe the phase separation of mixtures rapidly quenched to a temperature within the composition temperature envelope defined by the spinodal line. Phase separation proceeds initially by amplification of concentration fluctuations. Three features have generally been used to characterize spinodal decomposition: namely, (i) the appearance of well-defined, periodic concentration fluctuations; (ii) interconnectivity of phases; and (iii) a diffusion process where regions rich in one component get richer in that component with time.

Light scattering[1-5] and small-angle X-ray (SAXS)[6,16] and neutron (SANS)[17] scattering have been used to characterize the time-dependent changes in the concentration fluctuations. Typically, polymers develop concentration fluctuations up to the micron size scale, and hence, light scattering has been used predominantly to investigate kinetics of phase separation. According to the Cahn–Hilliard–Cook (CHC) linearized theory for rapid quenching of a mixture into the unstable region of the phase diagram,[3,10,12] the scattered intensity of light, $I(q,t)$ at a scattering vector q at a time t, is given by

$$I(q,t) = I(q,\infty) + (I(q,0) - I(q,\infty))e^{2R(q)t} \quad (1)$$

where $q = (4\pi/\lambda)\sin\theta$, λ is the wavelength, 2θ is the scattering angle, $R(q)$ is the amplification factor, and $I(q,\infty)$ is the "virtual" structure factor, the scattering characterizing an "equilibrium concentration fluctuation" at the quench temperature that would be observed if coarse phase separation did not occur. In other words, this is the structure factor for the case when the free energy of mixing is analytically continuous and has been extrapolated to the final quench temperature while the polymers remain randomly mixed. Equation 1 is expected to hold for only short times: $R(q)t < 1$. According to the linearized theory, $R(q)$ is given by

$$R(q) = -Dq^2 - 2M\kappa q^4 \quad (2)$$

where D is the diffusivity, M is the mobility, and κ is the interfacial free energy density. The diffusivity can be expressed as $M\partial f^2/\partial\phi^2$, where f is the free energy of mixing and ϕ is the concentration of one of the species. Equation 2 predicts a maximum in $R(q)$ at $q_{max} = (-D/4\kappa M)^{1/2}$ and a linear variation of $R(q)/q^2$ with respect to q^2.

The CHC theory of the phase separation is a mean-field theory and is valid only when concentration fluctuations are small. de Gennes[18] and Binder[12] have shown, for polymer blends in a melt, the conditions for the mean-field approximation to hold is given by

$$\bar{N}\left(1 - \frac{\chi_0}{\chi}\right) \gg 9\left(\frac{3}{4\pi}\right)^{4/3} \quad (3)$$

If χ is proportional to $1/T$, then eq 3 reduces to

$$\bar{N}\frac{T - T_c}{T_c} \gg 1 \quad (4)$$

where $\bar{N}$ is the average number of monomers per chain and T_c is the critical temperature. This inequality is easily satisfied for long polymer chains, whereas one must be much further away from T_c for simple liquids. Furthermore, high molecular weight polymers diffuse very slowly compared to simple liquids. Therefore, the short time region for which eq 1 holds is easily accessible. Together, both the mean-field behavior and the slow kinetics of high molecular weight polymer melts make them ideal materials for the study of spinodal decomposition.

It is the intent of this study to probe the effect of chain topology on the kinetics of phase separation by investigating mixtures of star-shaped molecules with linear molecules. In an earlier study,[19] we have found that the thermodynamics of the star/linear mixtures differ only slightly from their linear/linear counterpart. The question

0024-9297/90/2223-4452$02.50/0

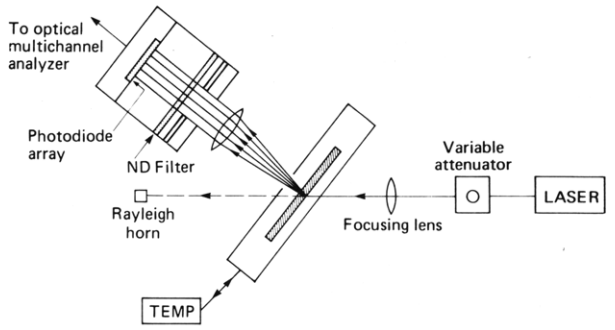

Figure 1. Schematic diagram of the light-scattering apparatus used in this study. Details are found in the text.

is whether or not the lack of reptative motion for star polymers at a high molecular weight of the arms[20,21] results in a significant change in the phase-separation kinetics.

Experimental Section

Mixtures of linear poly(vinyl methyl ether) (PVME) (M_w = 338 000, M_w/M_n = 1.69) with linear polystyrene (PS) (M_w = 600 000, M_w/M_n = 1.04 and M_w = 1 150 000, M_w/M_n = 1.09) and mixtures of four-armed star polystyrene (PS*) (M_w = 640 000, M_w/M_n = 1.03 and M_w = 1 050 000, M_w/M_n = 1.03) with arms of equal weight were cast from toluene solutions into cuvettes 100 μm in thickness. All polymers were synthesized, fractionated, and characterized in house. The cuvettes were left open in a vacuum oven at 80 °C for at least 4 h between successive measurements.

The light-scattering apparatus is shown in Figure 1. The light source was the 488-nm line of a vertically polarized Spectra Physics Model 165 Ar ion laser operated at 500-mW output. The light intensity from the laser was monitored by a photodiode and varied by less than one part in a thousand averaged over the course of a measurement. The light was attenuated by both neutral density filters and a variable attenuator by a factor of (2–5) × 10^4. A 30 cm focal length lens focussed the beam to a diameter of 0.5 mm. A Mettler FP83 heating stage with a hole for light passage was mounted in front of the focal point and controlled temperatures to an accuracy of 0.2° during measurements. The heating stage was rotated 20° from the position normal to the beam to allow scattering into a larger angular range. The detector, a 1024-pixel, linear photodiode array with intensifier plate, was interfaced with an EGG/PAR Model 1461 optical multichannel analyzer (OMA).[22] The OMA collected and stored both the scattered light intensity and the incident laser beam intensity during measurements and later transferred the data to an IBM PC/AT. The detector was mounted on a rotating arm. The apparent scattering angle was calibrated by use of diffraction gratings. The scattering angles in the sample were corrected for refraction at the sample surface. In terms of the corrected scattering vector, q, the three ranges used were 0.3–3.4, 1.8–4.6, and 3.5–6.3 μm^{-1} by positioning the rotating arm at three separate positions.

Linear temperature ramping was performed at several rates, from 0.5 to 2.0 °C/sec, to measure cloud points. The intensity integrated over 0.3–3.4 μm^{-1} in wavevector was plotted versus temperature. The cloud point was determined as the temperature at which the intensity deviated from the background. Results at different heating rates were extrapolated to a zero heating rate to yield the values of the cloud-point temperature[19] reported in Table I. Results from a previous study indicated that the critical composition was at a PS weight fraction of ca. 0.2 for both the linear/linear and the star/linear mixtures.[19]

Analysis of Scattering Data. Typical plots of the time dependence of the light scattering at the initial stages of the phase separation are shown in Figure 2. Two techniques were used to analyze the data for temperature jumps into the unstable region of the phase diagram. Both assume validity of the linearized theory as described in eq 1. From eq 1, it can be shown that[3]

$$\left(\frac{t}{I(q,t) - I(q,0)}\right)^{1/3} = ([I(q,\infty) - I(q,0)]2R)^{-1/3}(1 - Rt/3 + (Rt)^3/81 + ...) \quad (5)$$

For times such that $R(q)t < 1$, higher order terms are small so the linear approximation

$$\left(\frac{t}{I(q,t) - I(q,0)}\right)^{1/3} \approx ([I(q,\infty) - I(q,0)]2R)^{-1/3}(1 - Rt/3) \quad (6)$$

can be made. A linear least-squares fit for the data at short times where the RHS is plotted against time should, in principle, allow $I(q,\infty)$ and $R(q)$ to be easily determined. An example of such an analysis is shown in Figure 3 for a 13% PS* (M_w = 1.2 × 10^6) mixture with PVME quenched to 116 °C. In practice, however, such an interactive (experimental data on both sides of the equation) plot puts many stringent requirements on the experimental results. First, the procedure depends on the accuracy of the $I(q,0)$ values and the sharpness of the temperature jump, which usually takes about 60 s to reach the quench temperature. In this case, $I(q,0)$ was taken as an average over the first few points before the final temperature had been reached, and the starting time was the time when the quench temperature had been reached. Second, the relative noise was large at short times, since $I(q,t) - I(q,0)$ becomes small while the magnitude of the noise stays about the same. To reduce this noise, the data were first smoothed by using a five-point moving-average routine and then averaged over small angular ranges. This was limited to q values greater than 2 μm^{-1} due to a substantial contribution of background scattering at lower scattering vectors. Finally, a linear region had to be chosen to perform the least-squares fitting. One should notice that the linear time region decreases as q increases.

Alternatively, a Marquadt nonlinear mean least-squares regression[23] fit of eq 1 was used. For a specified region of data points, the routine solved for $I(q,0)$, $I(q,\infty)$, and $R(q)$ as well as the standard errors for all of these quantities. The absolute counting error was taken to be at least the square root of the number of counts. Figure 4, using the same data as Figure 3, is an example of a typical fit. The first point in the fit is the point where the final quench temperature was reached. The difficulty of this analysis is to decide what the maximum time is (after quench), which can still be considered in the linear region of spinodal decomposition. Since the nonlinear regression fit will automatically adjust $I(q,0)$, $I(q,\infty)$, and $R(q)$ to minimize the square deviation of the fit to experimental data, the true linear region may be narrower than the apparent one where experimental results clearly deviated from eq 1. For the same set of data and time range used in Figures 3 and 4, the values of $R(q)$ and $I(q,\infty)$ obtained are comparable. The results obtained by the nonlinear regression analysis will be used in the following discussion.

Discussion

The linearized CHC theory makes specific predictions on the dependence of $R(q)$ on q. In particular, from eq 2, $R(q)$ should exhibit a maximum at $q_{max}(-D/4M\kappa)^{1/2}$ and then be equal to zero at $q_c = (2q_{max})^{1/2}$. As q approaches zero, $R(q)$ should also extrapolate smoothly to zero. Finally, $R(q)/q^2$ must be a linear function of q^2 at scattering vectors less than $1/R_g$ where R_g is the radius of gyration.

From the analysis described, $R(q)$ was obtained as a function of q. Shown in Figure 5 are the data for a 20% PS* (M_w = 640 000) mixture with PVME quenched to 121 °C, which is 2 °C above the cloud-point temperature. It should be noted that the behavior of the linear/linear and star/linear mixtures was very similar in our experiments. Both are in qualitative agreement with the CHC theory; $R(q)$ extrapolates to zero at $q = 0$ and exhibits a maximum. The breadth of the curve, however, is broader than would be expected. Deviation from the CHC theory is also observed in plots of $R(q)/q^2$ versus q^2. As shown in Figure

Table I
Characteristics of Mixtures and Rates of Phase Separation

PS topology	ϕ_{PS}	$M_{PS} \times 10^{-5}$	T_Q[a]	T_s	q_{max}, μm^{-1}	$R(q_{max})$
linear	0.20	6.0	119.5	117.5	2.5 ± 0.5	1.0 ± 0.2
linear	0.20	6.0	121.5	117.5	2.5 ± 0.5	1.4 ± 0.2
star	0.20	6.4	119	117	4.2 ± 1.0	1.7 ± 0.3
linear	0.20	11.5	116	113.5	3.3 ± 0.5	0.8 ± 0.1
linear	0.20	11.5	118	113.5	4.0 ± 1	1.3 ± 0.2
star	0.25	10.5	116	114	3.0 ± 0.8	0.4 ± 0.1
star	0.25	10.5	118	114	4.1 ± 1.0	0.9 ± 0.1
star	0.13	10.5	116	114.5	3.0 ± 0.8	0.8 ± 0.1

[a] T_Q is the quench temperature.

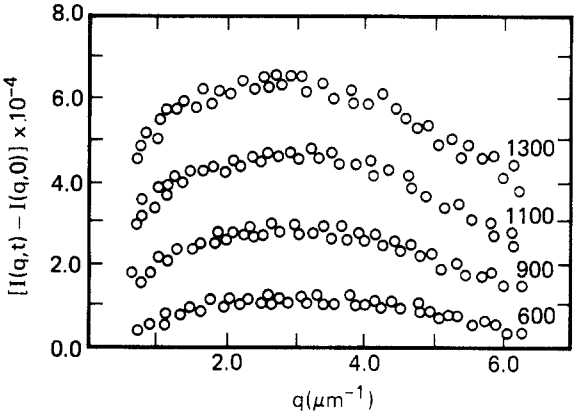

Figure 2. Time dependence of the light scattering for a mixture of 20% four-armed star polystyrene (M_w = 640 000) with PVME quenched to 121 °C. The time indicated on the right-hand side is in seconds. The intensity shown in that in excess of the initial fluctuation scattering.

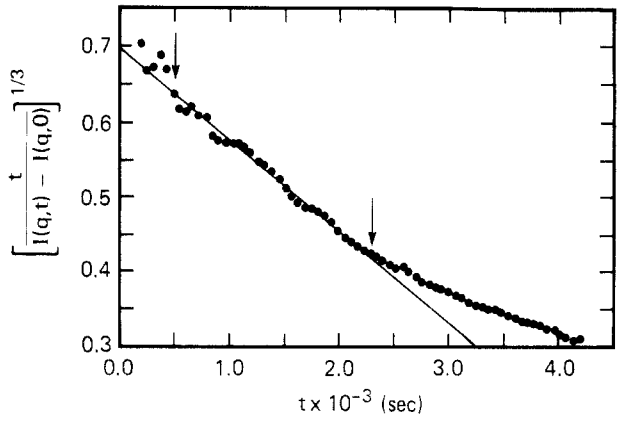

Figure 3. Light scattering for a mixture of 13% four-armed polystyrene (M_w = 1 050 000) with PVME quenched to 116 °C at q = 5.8 μm^{-1} analyzed in accordance with eq 5. The arrows indicate the time range where the fitting procedure was used.

6 for the 20% PS* (M_w = 640 000) mixture quenched to 121 °C, pronounced curvature in the data is observed. Since both the star/linear and linear/linear mixtures exhibit these deviations with a similar magnitude, it is apparent that the chain topology does not change the phase-separation kinetics of binary polymer mixtures. Most reported studies of the early stage of spinodal decomposition have resulted in a curved $R(q)/q^2$ versus q^2 plot. The recent study of Sato and Han[3] has attributed this to the omission of the $I(q,\infty)$ term in eq 1 and to the inability to obtain truly early stage data with enough precision in most systems studied. All experimental results are consistent with the notion that CHC linearized theory is only quantitatively correct for a very short time range. Qualitative features can be extracted by using CHC theory for a wider, more generally accessible time range. Deviations due to the nonlinearities that have been omitted in

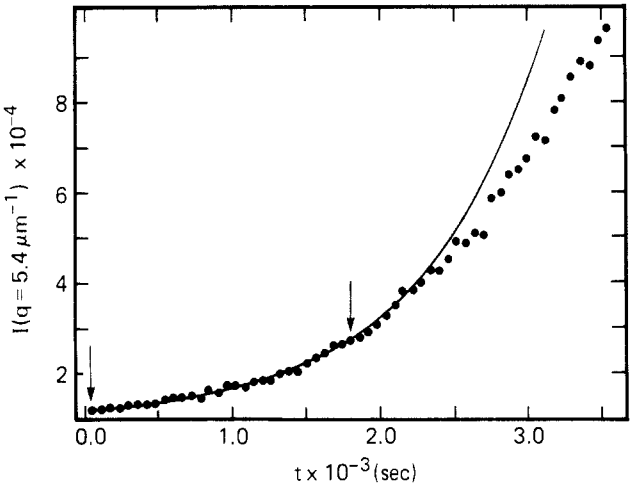

Figure 4. Same data as in Figure 3 analyzed by using a Marquadt nonlinear mean least-squares regression. The arrows indicate the time range where the fitting procedure was used.

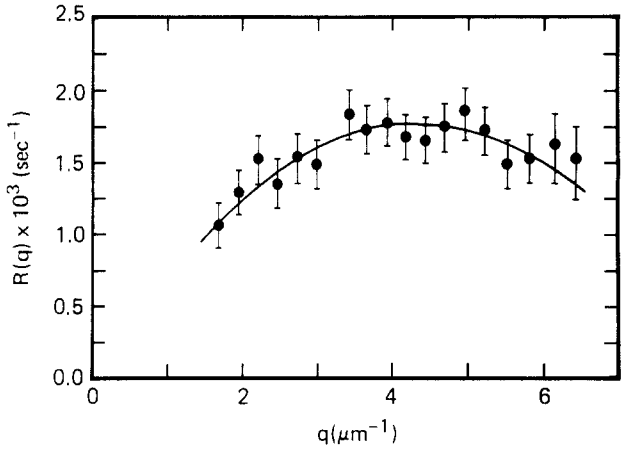

Figure 5. Amplification factor $R(q)$ for a 20% mixture of four-armed star polystyrene (M_w = 640 000) with PVME quenched to 121 °C approximately 2 °C above the spinodal. The error limits were those obtained for the nonlinear regression.

the linearization of the diffusion equation have caused discrepancies between observations and CHC predictions.

As far as the chain topology is concerned, the effect is more evident in the maximum values of the amplification factor. Since the q range where $R(q)$ is near its maximum is rather broad, $R(q_{max})$ can be evaluated with a fair degree of precision. These data are shown in Table I. For the purpose of comparison the data have been arranged according to the total molecular weight. For the linear/linear mixtures of PS (M_w = 600 000), the expected increase in $R(q_{max})$ is observed by increasing the quench temperature by 2 °C. However, for a similar quench temperature, albeit different quench depths from the cloud point, $R(q_{max})$ does not vary with the chain topology. If anything, $R(q_{max})$ is slightly greater for the star/linear mixture than for the

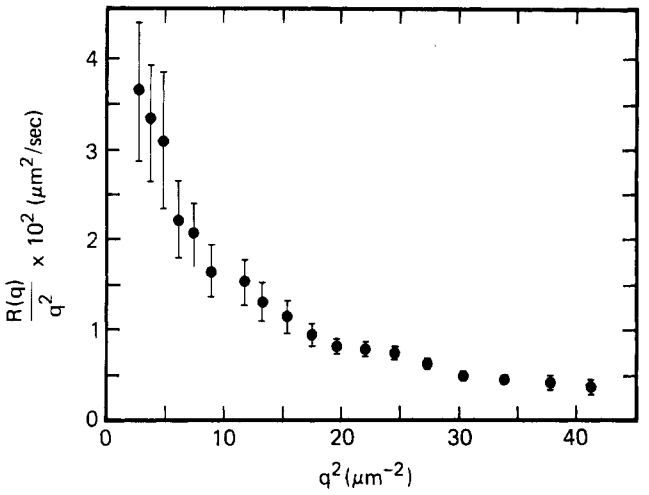

Figure 6. $R(q)/q^2$ as a function of q^2 for a 20% mixture of four-armed star polystyrene (M_w = 640 000) with PVME quenched to 121 °C.

linear/linear mixture. The result is not too surprising since the effect of the arms is not significant for these lower molecular weight polymers. In fact, this is consistent with the study of self-diffusion coefficients of star and linear polystyrene in PVME matrices by Lodge et al.[24]

Increasing the molecular weight brings about marked differences between the linear/linear and star/linear mixtures. Comparison of quenches to the same temperature shows that $R(q_{max})$ for the star/linear mixture is at least 30% lower than that of the corresponding linear/linear mixtures. This difference is magnified slightly since the star/linear systems contain ca. 5% more polystyrene, the higher glass transition component. The cooperative nature of the phase separation is exemplified by the data for the 13% PS* (M_w = 1 050 000) mixture where the reduced polystyrene concentration brings about a marked increase in $R(q_{max})$ such that it is similar to that observed for the linear/linear mixture containing 20% polystyrene.

In summary, it has been shown that the phase separation of star/linear mixtures is essentially the same as that of linear/linear mixtures. The effect of arm retraction is only evident for the highest molecular weight star polymers studied. For both mixtures, the linearized CHC theory only qualitatively describes the experimental data. We believe this is caused by the nonlinear effects, which become important very early in the spinodal decomposition process of binary polymer mixtures.

References and Notes

(1) Izumitani, T.; Hashimoto, T. *J. Chem Phys.* **1985**, *83*, 3694.
(2) Snyder, H. L.; Meakin, P.; Reich, S. *Macromolecules* **1983**, *16*, 757.
(3) Sato, T.; Han, C. C. *J. Chem. Phys.* **1988**, *88*, 2057.
(4) Okada, M.; Han, C. C. *J. Chem. Phys.* **1986**, *85*, 5317.
(5) Kumaki, J.; Hashimoto, T. *Macromolecules* **1986**, *19*, 763.
(6) Meier, H.; Strobl, G. R. *Macromolecules* **1987**, *20*, 649.
(7) de Gennes, P. G. *J. Chem. Phys.* **1980**, *72*, 4756.
(8) Pincus, P. *J. Chem. Phys.* **1981**, *75*, 1996.
(9) Heerman, D. W. *Phys. Rev. Lett.* **1984**, *52*, 1126.
(10) Strobl, G. R. *Macromolecules* **1985**, *18*, 558.
(11) Ronca, G.; Russell, T. P. *Phys. Rev. B* **1987**, *35*, 8566.
(12) Binder, K. *J. Chem. Phys.* **1983**, *79*, 6387.
(13) Cahn, J. W. *J. Chem. Phys.* **1965**, *42*, 93; Cahn, J. W. *Trans. Met. Soc. AIME* **1968**, *242*, 166.
(14) Hilliard, J. E. Spinodal Decomposition. In *Phase Transformations*; Aronson, H. I., Ed.; American Society for Metals: Metals Park, OH, 1970.
(15) Cook, H. E. *Acta. Metall.* **1970**, *18*, 297.
(16) Russell, T. P.; Hadziioannou, G.; Warburton, W. *Macromolecules* **1985**, *18*, 78.
(17) Schwahn, D.; Springer, T.; Mortensen, K.; Yee-Madeira, H. *Dynamics of Ordering Processes in Condensed Matter*; Komura, S., Furakawa, H., Eds.; Plenum Press: New York, 1987.
(18) de Gennes, P.-G. *J. Phys. Lett.* **1986**, *85*, 3556.
(19) Russell, T. P.; Fetters, L. J.; Clark, J. C.; Bauer, B. J.; Han, C. C., accepted for publication in *Macromolecules*.
(20) de Gennes, P.-G. *J. Phys. (Paris)* **1975**, *36*, 1199.
(21) Roovers, J. *Macromolecules* **1987**, *20*, 148.
(22) Certain commercial materials and equipment are identified in this paper in order to specify adequately the experimental procedure. In no case does such identification imply recommendation or endorsement by the National Institute of Standards and Technology.
(23) Bard, Y. *Nonlinear Parameter Estimation*, Academic Press: New York, 1974.
(24) Lodge, T. P.; Wheeler, L. M. *Macromolecules* **1986**, *19*, 2983.

Registry No. PVMe, 9003-09-2; PS, 9003-53-6.